Solar Energy 146 (2017) 287–297

Contents lists available at ScienceDirect

Solar Energy

journal homepage: www.elsevier.com/locate/solener

Atmospheric-pressure plasma surface activation for solution processed photovoltaic devices

F. Lisco, A. Shaw, A. Wright, J.M. Walls *, F. Iza

Wolfson School of Mechanical, Electrical and Manufacturing Engineering, Loughborough University, Loughborough LE11 3TU, United Kingdom

ARTICLE INFO

Article history:
Received 11 August 2016
Received in revised form 15 February 2017
Accepted 19 February 2017

Keywords:
Atmospheric plasma
Cadmium sulphide thin films
Photovoltaic devices
Surface energy
Surface contamination
Atmospheric deposition processes

ABSTRACT

Atmospheric solution based processes are being developed for the fabrication of thin film photovoltaic devices. Deposition techniques such as electrodeposition, spin coating, spraying or printing are promising techniques to increase the throughput and reduce the cost per Watt of Copper-Indium-Gallium-Selenide (CIGS), Copper-Zinc-Tin-Sulphide (CZTS) and perovskite thin film solar technologies. All these technologies require pre-treatment of the substrate prior to the deposition of the thin film and ideally this pre-treatment should also be performed at atmospheric pressure. Results presented in this paper show that use of an atmospheric-pressure plasma is highly effective in activating the surface of substrates commonly used in thin film photovoltaic (PV) device fabrication. Surface activation improves the adhesion of thin films. The use of an atmospheric activation process is compatible with a continuous vacuum-free PV fabrication process. Soda lime glass (SDL) and fluorine doped tin oxide (FTO) coated glass are substrates commonly used in the fabrication of photovoltaic modules. These substrates have been surface treated using a He/O_2 atmospheric-pressure plasma, resulting in increased surface energy as evidenced by Water Contact Angle (WCA) measurements. The pre-treatment reduces adventitious surface contamination on the substrates as shown using X-ray Photoelectron Spectroscopy (XPS) measurements. The advantages of using the atmospheric plasma surface pre-treatment has been demonstrated by using it prior to atmospheric deposition of Cadmium Sulphide (CdS) thin films using a sonochemical process. The CdS thin films show pinhole-free coverage, faster growth rates and better optical quality than those deposited on substrates pre-treated by conventional wet and dry processes.

1. Introduction

Reducing the cost of energy is a major driving force in solar energy research as it leads directly to increased deployment of photovoltaic (PV) modules. Reduction of the cost of energy can be achieved either by increasing the efficiency of devices or by reducing the cost of manufacturing. Thin film photovoltaics hold out the promise of reducing the cost of solar energy because thin film modules inherently use less material than conventional crystalline silicon modules and the manufacturing methods involve fewer and less energy intensive fabrication steps (Baldwin et al., 2015). It is possible to reduce current fabrication costs further if expensive vacuum based deposition techniques could be replaced by atmospheric-pressure fabrication methods. As a result, research is being carried out to develop atmospheric deposition processes such as electrodeposition (Deligianni et al., 2011), spin coating (Zhang et al., 2014; Mitzi et al., 2008), chemical bath deposition (Wangperawong et al., 2011), spraying (Arnou et al., 2016) or printing (Suryawanshi et al., 2013) to reduce the cost per Watt peak (Wp) of CIGS, CZTS and perovskite thin film solar technologies.

There is no practical alternative to using a wet chemistry cleaning method such as the RCA process (Franssila, 2005) to remove gross surface contamination and particulates. However, these techniques do not create a highly activated surface because adventitious carbon contamination from the atmosphere remains. Also, wet treatments can leave residues on the surface. Hence it is necessary to remove this thin layer of contamination to improve the subsequent adhesion of the thin film. Several techniques have been used for surface activation such as ultraviolet ozone treatments UV/O_3 (Hachioji-shi, 1987), dry CO_2 (Sherman et al., 1994) and low-pressure vacuum plasmas (Slyke et al., 1996; Low et al., 2002; Kim et al., 2002; Swanson et al., 2012).

Low-pressure vacuum plasma cleaning is a well-established process widely used prior to thin film deposition. In addition to removing contaminants, the process increases the surface energy of the substrate and this promotes the adhesion of the thin film

* Corresponding author.
E-mail address: j.m.walls@lboro.ac.uk (J.M. Walls).

http://dx.doi.org/10.1016/j.solener.2017.02.030
0038-092X/

and reduces pinhole formation (Lisco et al., 2014). Low-pressure vacuum plasma systems require relatively low voltages to ignite and sustain the plasma. However, the use of a vacuum chamber and pumps is needed to maintain low working gas pressure during the process. These vacuum systems require significant capital expenditure and regular maintenance, making low-pressure vacuum plasma processes quite costly. In addition to the cost, moving substrates in and out of vacuum is also slow and disrupts the manufacturing process flow.

In recent years, atmospheric-pressure plasmas such as corona discharges (Samanta et al., 2006), plasma torches (Fauchais and Vardelle, 1997), dielectric barrier discharges (DBD) (Belkind and Gershman, 2008), Radio Frequency (RF) plasmas (Morent et al., 2008) and microwave plasmas (Thejaswini et al., 2014) have been developed for a number of application areas including textiles (Morent et al., 2008), metallurgy (Schutze et al., 1998), water treatment (Foster et al., 2012; Kogelschatz, 2003), biomedical applications (Woedtke et al., 2013; Walsh et al., 2006; Iza et al., 2008), food industry applications (Shaw et al., 2015) and material processing (Thejaswini et al., 2014; Selwyn et al., 2001; Mariotti et al., 2016; Cheng et al., 2011; Massines et al., 2012). For example, atmospheric diffuse co-planar surface barrier discharge (DCSBD) have been used for surface cleaning of indium-tin-oxide (ITO) for microelectronic device manufacturing (Homola et al., 2012). Four approaches are typically combined in these atmospheric-pressure plasma systems to maintain the non-thermal character of the plasma despite the high collisionality encountered at atmospheric pressure (Iza et al., 2008): (1) large flows, (2) dilution of molecular gases in noble gases (e.g. He, Ar), (3) small scale discharges to take advantage of large surface to volume ratios and (4) pulsed operation to prevent thermalisation of the discharge. The latter can be achieved either by pulsing the input voltage to the plasma source or by introducing dielectric barriers that quench the plasma at each cycle.

In this paper, we report on the use of a He/O_2 atmospheric-pressure dielectric barrier discharge as a dry plasma cleaning and surface activating pre-treatment process for atmospheric-deposition of CdS thin films. Thin film CdS is often used as an n-type window layer in thin film PV devices. It is shown that the activation treatment improves the optical, morphological and structural properties of the CdS thin films. The plasma-induced surface energy and chemical modification of soda lime glass (SDL) and fluorine doped tin oxide (FTO) coated glass has been characterised using water contact angle (WCA) measurements and X-ray photoelectron spectroscopy (XPS). In addition, the optical and morphological quality of CdS thin films deposited on plasma-treated substrates has been characterised using ultraviolet and visible spectrophotometry, spectroscopic ellipsometry (SE), optical microscopy and scanning electron microscopy (SEM).

2. Materials, methods and experimental set-up

2.1. Glass substrates

TEC 10 glass supplied by NSG-Pilkington and soda lime (SDL) glass are materials commonly used as substrates for thin film PV fabrication. TEC 10 is a multilayer stack consisting of a layer of 25 nm SnO_2 layer, 25 nm SiO_2 layer and a top layer of ~400 nm thick electrically conducting layer of fluorine doped tin oxide (SnO_2:F), deposited on a 3.2 mm thick glass. TEC 10 has a sheet resistance of ~10 Ω/□ and high transparency with ~83% average light transmittance [http://www.pilkington.com/products]. These are the typical electrical and optical properties required for a PV device substrate. The SDL glass used in this work is a standard 1 mm thick slide manufactured from extra white glass with the following approximate chemical composition: SiO_2 72.2%, Na_2O 14.30%, K_2O 1.20%, CaO 6.40%, MgO 4.30%, Al_2O_3 1.20%, Fe_2O_3 0.03% and SO_3 0.30% ("Menzel-Gläser_Microscope Slides," n.d.).

Both the TEC 10 and SDL substrates were treated with the atmospheric-pressure plasma and their surface chemical composition was studied before and after the atmospheric plasma treatment. The substrate size was 5×5 cm^2 and the surface area was fully treated. CdS thin films were deposited on TEC10 by sono-chemical bath deposition (sonoCBD). Details of this deposition process have been reported elsewhere (Lisco et al., 2014).

Both TEC10 and SDL are important substrates for thin film photovoltaics. For example, TEC10 is commonly used for thin film CdTe and perovskite solar cells in the superstrate configuration. SDL glass is used for CIGS and CZTS devices in the substrate configuration.

2.2. Water contact angle

Measuring the water contact angle (WCA) of a de-ionised water droplet on a surface is a widely used technique to quantify the wettability of a surface and its cleanliness (Lee et al., 2007). An OCA-20 Dataphysics water contact angle measuring instrument was used in this study to measure the surface energy and wettability of substrates before and after atmospheric plasma treatment. 1 μL of de-ionised water was dispensed for each measurement, 10 measurements were performed for each sample and the mathematical average was used in the results section. The presence of adventitious organic contamination reduces surface energy and increases the water contact angle. Therefore, removal of this contamination results in a decrease in the observed contact angle. A highly activated surface will correlate with a significant spread of the water droplet with very low contact angle. Adventitious carbon from the atmosphere re-contaminates the surface and the speed of this process has been monitored with repeated WCA measurements over time.

2.3. Chemical surface composition

X-ray photoelectron spectroscopy (XPS) surface analysis was used to obtain the chemical composition of the plasma treated glass surfaces and the deposited CdS thin films. The analysis was performed using a Thermo Scientific K-Alpha XPS instrument. An electron flood gun was used to reduce charging that would otherwise cause peak shifts to occur. The binding energies were calibrated based on the position of the C1s peak at 284.8 ± 0.2 eV as a reference. The X-ray source used Al K_α radiation at $h\nu$ = 1486.6 eV

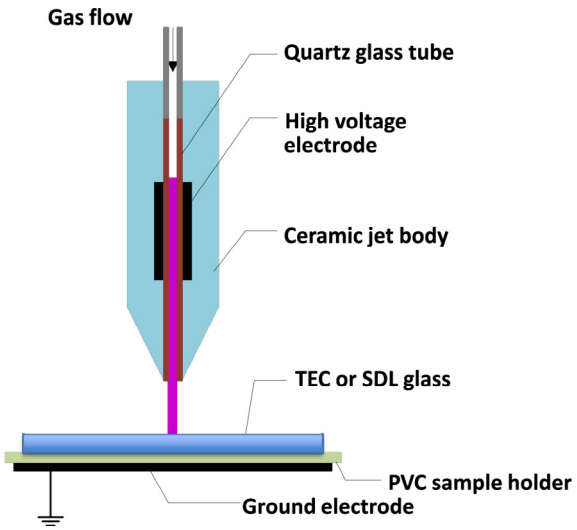

Fig. 1. Schematic diagram of the atmospheric pressure plasma jet used in this work.

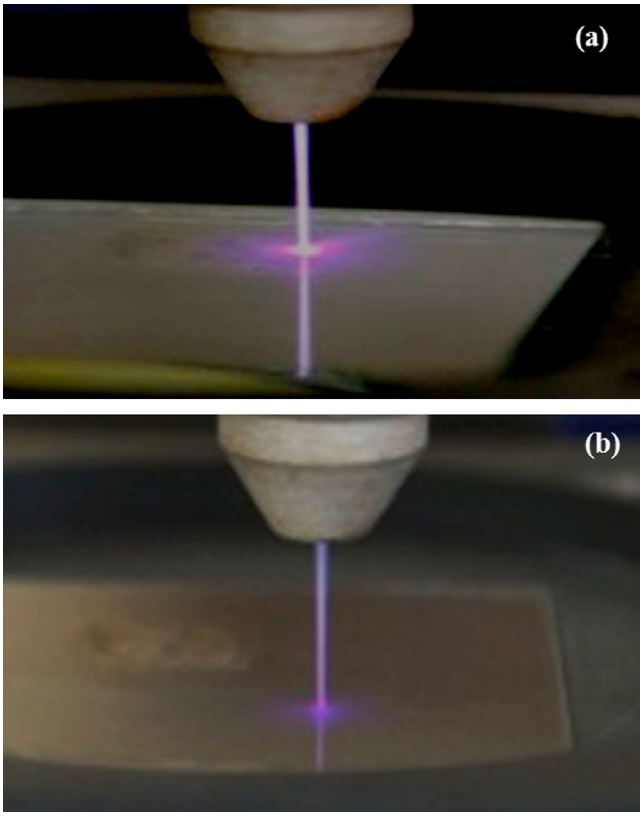

Fig. 2. The atmospheric-pressure plasma treating conductive TEC10 fluorine doped tin oxide coated glass surface (a) and insulating soda lime glass (b). Note that the plasma jet spreads over a larger area on the electrically conducting surface.

with a beam diameter of 200 μm. High resolution multiplex scans were used to evaluate the chemical state(s) of C1s, O1s, Sn3d, Cd3d and S2p photoelectron core levels. The F1s peak (from the SnO_2:F) is not included in the analysis because at the low doping level used, the signal is too low in intensity to be resolved. Precise determination of binding energies was made through the use of deconvolution curve fitting routines applied to the peaks in the multiplex scan and sensitivity factors were used to determine elemental composition.

2.4. Optical properties

CdS thin films were deposited on atmospheric-plasma treated TEC10 substrates to assess the compatibility and efficacy of the treatment for PV device fabrication. The transmission and the band gap energy of the CdS thin films were measured using a spectrophotometer (Varian Cary® UV–Vis 5000) equipped with an integrating sphere and a set of gratings which allow the collection of transmission measurements for wavelengths in the range from 185 nm to 3.3 μm. The samples were placed in the spectrophotometer over the entrance port of the integrating sphere with the uncoated glass surface facing the light source. This configuration is appropriate for measuring the transmission through a superstrate CdTe/CdS solar cell. The band gap energy (E_g), was obtained as a graphic extrapolation using a Tauc plot (Rakhshani, 2000) based on the following relationship:

$$\alpha = \frac{A(h\upsilon - E_g)^p}{h\upsilon} \quad (1)$$

where α is the absorption coefficient, A a proportionality constant, E_g the band gap energy, ν the light frequency, h the Plank constant and p a numerical coefficient that depends on the material properties. For direct band gap materials such as CdS, p is equal to 0.5.

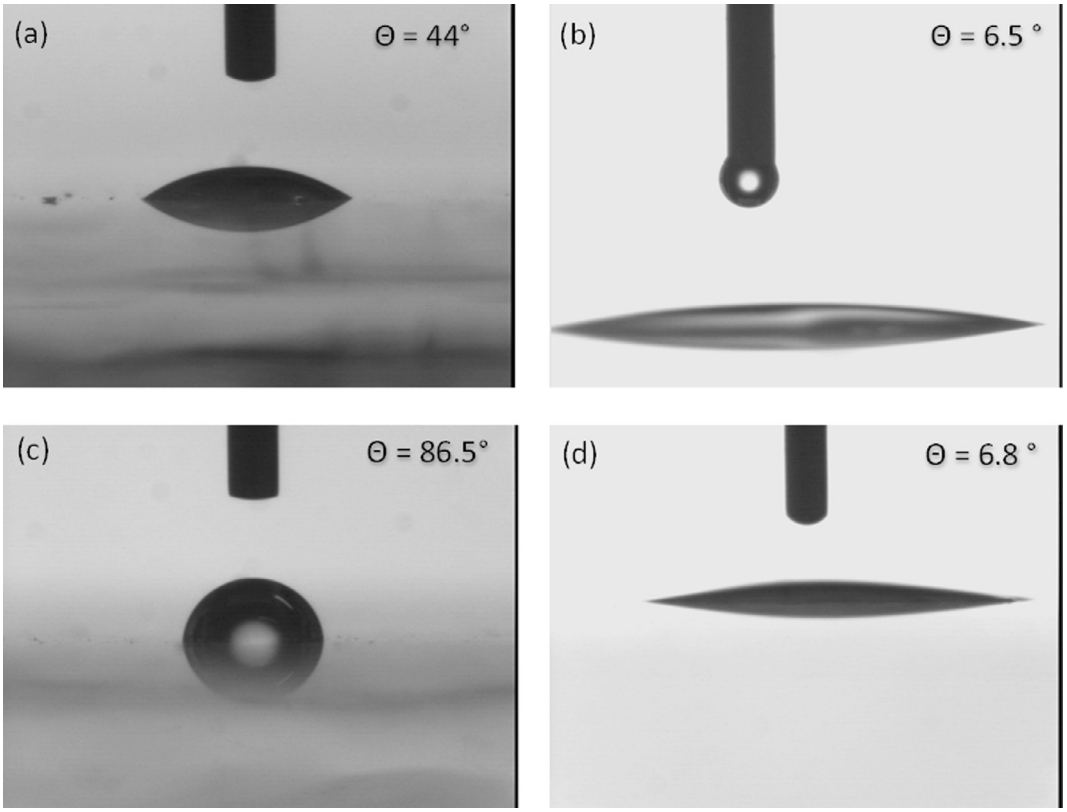

Fig. 3. Water contact angle (WCA) images of a sodalime glass surface before (a) and after (b) the atmospheric plasma treatment and a TEC10 glass surface before (c) and after (d) the atmospheric plasma treatment.

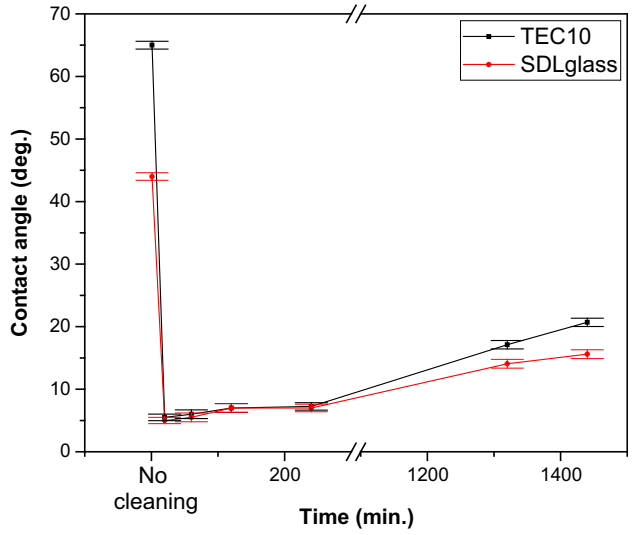

Fig. 4. WCA measurements with error bars against time show the ageing effect of the atmospheric-pressure treatment on TEC10 and sodalime glass surfaces.

The optical constants of the CdS thin films were measured using spectroscopic ellipsometry (SE) (Horiba, Jobin Yvon, UVISEL). A multi-layer model consisting of TEC-substrate/interface/CdS-film/surface-roughness/air was used to analyse the ellipsometry data and derive the refractive index (n), extinction coefficient (k), and thickness of the CdS thin films. The dispersion of the refractive index and extinction coefficient was measured in the wavelength range from 248 nm to 2100 nm. The optical properties of the TEC10 substrate were determined separately prior to the CdS deposition. The TEC10/CdS interface was then modelled as a Bruggeman effective medium (BEMA) (Gonçalves and Irene, 2002). The optical properties of the CdS film were parameterised using a double Tauc Lorentz dispersion formula (Fujiwara, 2007):

$$\varepsilon_r(E) = \varepsilon_r(\infty) + \sum_{i=1}^{N} \frac{2}{\pi} \cdot P \cdot \int_{E_g}^{\infty} \frac{\xi \cdot \varepsilon_i(\xi)}{\xi^2 - E^2} d\xi$$

$$\varepsilon_i(E) \begin{cases} \sum_{i=1}^{N} \frac{1}{E} \times \frac{A_i \cdot E_i \cdot C_i \cdot (E-E_g)^2}{(E^2-E_i^2)^2 + C_i^2 \cdot E^2} & \text{for } E > E_g \\ 0 & \text{for } E \leqslant E_g \end{cases} \quad (2)$$

where ε_r is the real part of the dielectric function, ε_i the imaginary part, A_i the Tauc coefficient, E the photon energy, E_i the transition energy of the oscillator of highest order, C_i the broadening term of the peak, and E_g the optical band gap. The roughness layer in

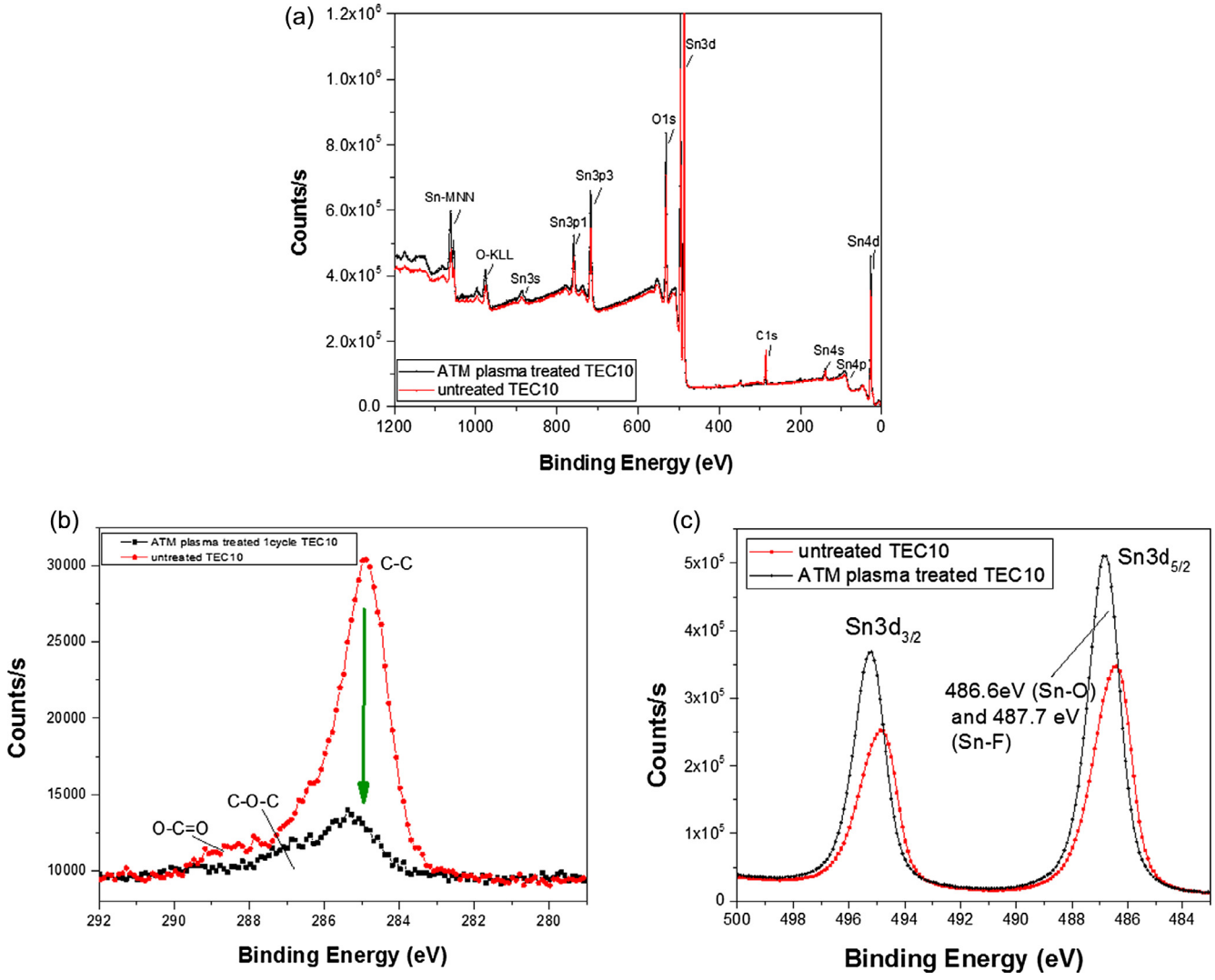

Fig. 5. XPS survey scan (a), high resolution analysis of C1s peak (b) and $Sn3d_{3/2}$, $Sn3d_{5/2}$ peak (c) for the untreated and atmospheric-pressure treated TEC10 sample.

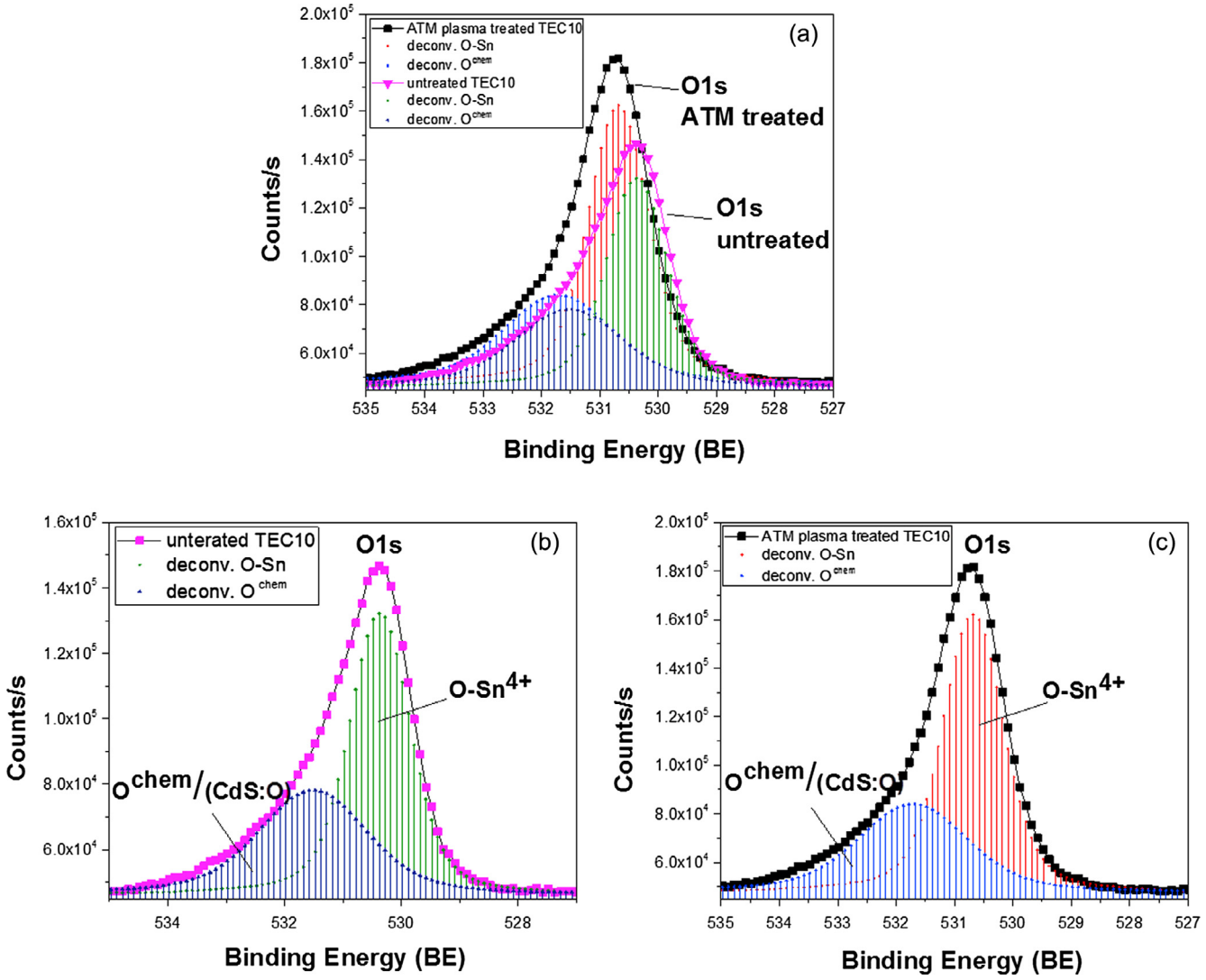

Fig. 6. XPS high resolution analyses of O1s peaks for untreated and atmospheric-pressure plasma treated TEC10 glass. O peaks deconvoluted into their two components, chemisorbed O and O–Sn (a). XPS high resolution with the deconvolution of the two components of O1s for untreated (b) and ATM plasma treated TEC10 glass (c).

the ellipsometry multilayer model incorporates the effect of the superficial oxidation of the films (see XPS analysis below). The roughness layer was modelled using a modified dispersion law of the CdS layer.

2.5. Surface morphology measurements

The surface morphology of the deposited CdS thin films was studied with a high resolution field emission gun scanning electron microscope (FEG-SEM), Leo 1530 VP FEG-SEM, which provides the ability to image surface features with nanometre resolution.

Pinholes are microscopic imperfections in the thin film which appear as pits or holes visible on the surface and through the layer. Pinholes are a common problem in thin-film CdS when used in PV devices (Lisco et al., 2014). In this study, optical microscopy was used to detect the presence of these defects. A Lumenera Infinity 1–3 Digital Camera with Infinity Analyse software was used to collect images with advanced camera control and image processing. An objective magnification of 100× was used with a working distance of 0.13 mm and a numerical aperture (N.A.) 1.25 with a resolution of 0.27 μm. AxioVision LE64 software was used to quantify the size of pinhole defects in the CdS layers and also to measure the grain size of CdS films.

2.6. Conventional cleaning methods

Results were compared with conventional cleaning methods to assess the efficacy of the proposed atmospheric-pressure plasma cleaning process. Dry cleaning was performed using a low-pressure vacuum (~300 mTorr) Ar/O_2 plasma. Substrates were plasma treated for 5 min in a parallel plate plasma reactor, Glen100-P AE Advanced Energy, using 20 sccm O_2/30 sccm Ar. We performed a process previously optimised in our laboratory, details of the process are provided elsewhere (Lisco et al., 2014). Also for comparison, substrates were wet cleaned for 5 min in an ultrasonic bath with isopropanol alcohol (IPA) (Sigma–Aldrich) and de-ionised water (Milli-pore), in the ratio 1:10.

2.7. Atmospheric-pressure plasma setup

The plasma source used in this work is a dielectric barrier discharge (DBD) plasma jet operating at 14.16 kHz, 10 kV. The power consumed by the plasma is typically less than 10 W. The jet consists of a quartz tube with an inner diameter of 1.5 mm and a metallic high voltage electrode wrapped tightly around the quartz tube (Fig. 1). The ground electrode is positioned beneath a PVC sample holder and the plasma is driven by an in-house built

half-bridge resonant power supply. The jet is located at a distance of 1 cm above the substrate being treated, as shown in Fig. 1. In this jet, the electric field between the wrapped ring electrode and the ground electrode is largely in the axial direction, parallel to the carrier gas flow through the quartz tube (Walsh et al., 2010). The TEC10 substrate with its transparent conducting layer was allowed to float electrically. The atmospheric-pressure plasma jet is a versatile plasma device that can be operated on a large variety of substrates including planar and non-planar substrates, conducting and insulating substrates, and rigid and flexible polymeric substrates.

A mixture of helium (3 standard litres per minute – slm) and oxygen (15 standard cubic centimetres per minute - sccm) is used as the carrier gas for the plasma and mass flow controllers (MKS 1179A) were employed to provide a constant gas flow during the duration of the treatment. This gas mixture combines the properties of both He and O_2. The high thermal conductivity of helium maintains the gas temperature close to room temperature, preventing the onset of thermal instabilities. The oxidative power of oxygen-derived species, such as atomic oxygen, singlet oxygen and ozone (Liu et al., 2010), is critical for cleaning and activating glass surfaces. The ionised helium-oxygen admixture forms a plasma plume that extends beyond the glass tube into the surrounding ambient air and reaches the surface under treatment (Fig. 1 and Fig. 2).

A programmable XY-translation stage is moved to scan the substrates beneath the plasma, ensuring even and repeatable plasma treatments. The stage describes a grid pattern at 1 mm intervals at a speed of 40 mm/s, taking ~40 s to treat a 5 cm × 5 cm substrate surface.

Since the glass sample forms part of the electrical circuit of the system, the plasma depends on the electrical properties of the substrate being treated even if the same applied voltage and the same He-O_2 flow rate are used for all experiments. As shown in Fig. 2, the plasma jet appears more intense and brighter when an electrically conducting surface such as TEC10 glass is used (Walsh et al., 2006).

3. Results and discussion

3.1. Activation of soda lime (SDL) and TEC10 glass surfaces

The effect of a single cycle of atmospheric-pressure plasma treatment (3 slm He and 15 sccm O_2) on the water contact angle (WCA) of SDL and TEC10 glass substrates is shown in Fig. 3. The substrates were used, as received, after being rinsed with deionised water and dried using pressurised nitrogen gas. The low wettability of the substrates before the plasma treatment (~44° and ~86° for the SDL and TEC10 substrates respectively) was significantly improved by the atmospheric plasma treatment, which reduced the WCA to values less than 10°.

The decrease in WCA shown in Fig. 3 was retained even after exposing the samples to open air for several hours. The slow recovery over time of the WCA for plasma treated SDL and TEC10 glasses is shown in Fig. 4. The WCA reduced dramatically for both substrates during the plasma treatment and increased only gradually over time with exposure to the atmosphere. Even 300 min after the plasma treatment, the WCA remained below 10° for both surfaces. After exposure to atmosphere for 1 day the WCA remained below 20°.

3.2. Effect of atmospheric-pressure plasma treatment on the surface composition of TEC10 substrates

XPS analysis was performed on untreated and treated TEC10 substrates and the relative concentration of carbon, tin and oxygen was analysed (Fig. 5(a)). The presence of carbon is undesirable and is a result of adventitious atmospheric carbon dioxide, carbon monoxide and organic contamination. After one cycle of atmospheric-pressure plasma treatment, the XPS scan of the C1s peak at 285 eV showed a dramatic decrease in intensity, with the

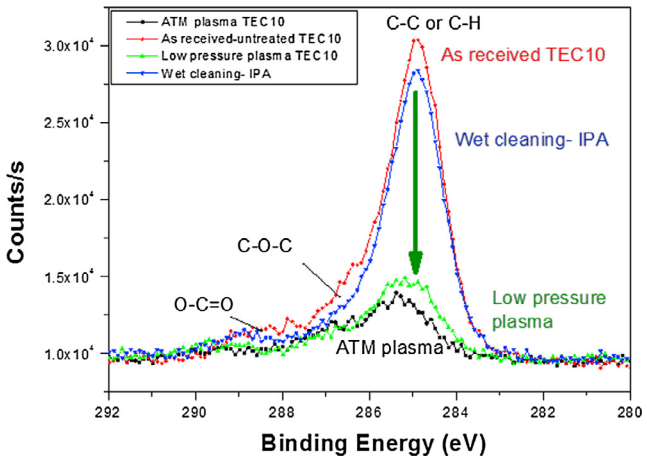

Fig. 7. XPS high resolution analysis of C1s peak for as received TEC10, 5 min IPA ultrasound cleaned TEC 10, 5 min low-pressure plasma treated TEC10 and 40 s atmospheric-pressure plasma treated TEC10 glass.

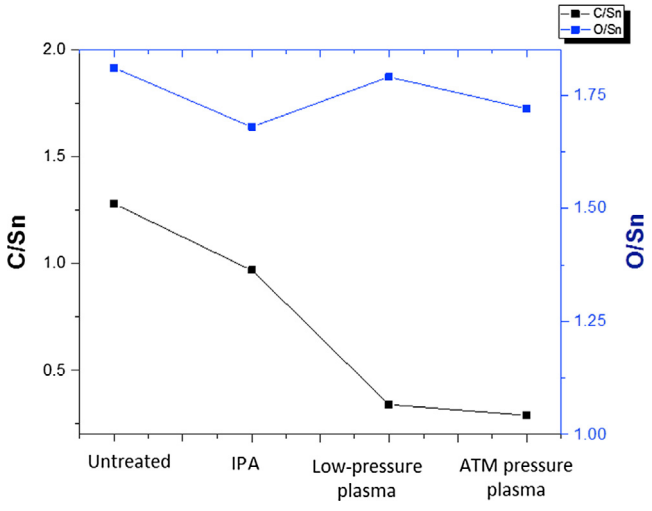

Fig. 8. A comparison of XPS C/Sn and O/Sn ratios for a TEC 10 surface without surface activation, treated by wet cleaning with IPA, low-pressure vacuum plasma and ATM pressure plasma treatments.

Table 1
Atomic percentages of C, Sn and O species detected by XPS high resolution analysis on the untreated, IPA wet cleaned, low pressure vacuum plasma and atmospheric-pressure plasma treated samples of TEC10 glass.

	Untreated TEC10	IPA ultrasound cleaning (5 min)	Low-pressure plasma (5 min)	Atmospheric-pressure plasma (40 s)
C1s (At%)	31.3	26.6	10.7	9.6
Sn3d5 (At%)	24.4	27.4	31.5	32.9
O1s (At%)	44.2	46	56.6	56.6

carbon concentration being reduced from 31 At% to 9.6 At% (Fig. 5). This reduction in the surface carbon concentration demonstrates that atmospheric-pressure plasma treatment can be an effective procedure for removing organic contamination. Also shown in Fig. 5 is the high resolution $Sn3d_{5/2}$ XPS peak, which corresponds to Sn^{2+} (485.9 eV) and Sn^{4+} (486.6 eV). The intensity of this peak increases and slightly shifts after the plasma treatment due to the removal of surface contaminants. This slight shift towards higher energies is due to a change in the band bending of the semiconducting oxide surface after the removal of the adsorbates.

XPS has also been used to study the effect of the atmospheric-pressure plasma on the oxygen content on the surface. Fig. 6 shows a comparison between the O1s oxygen peak of the untreated TEC10 surface and that of the surface treated with atmospheric-pressure plasma. The O1s oxygen peak observed in the high resolution XPS is the superposition of two main components. The first component is located at a binding energy (BE) of 530.5 eV and corresponds to O-$Sn^{4+/2+}$ (NIST database ("NIST X-ray Photoelectron Spectroscopy Database, Version 4.1," 2012)), and the other component located at a BE ~ 532 eV is attributed to oxygen atoms chemisorbed at the surface (O^{chem} (Kwoka et al., 2005)) and/or CO bonds from the contaminants.

3.3. Comparison of cleaning procedures

The results presented in the previous sections indicate that atmospheric-pressure plasma removes organic contaminants and activates the TEC10 surface. In this section, the efficacy of the atmospheric-pressure plasma treatment is compared to conventional cleaning processes, using low-pressure Ar/O_2 plasma and isopropyl alcohol (IPA) ultrasound wet cleaning.

The XPS analysis of the C1s peak for each cleaning process is shown in Fig. 7. Additional analysis of Sn3d and O1s peaks is provided in Table 1. Fig. 8 shows the C/Sn ratio used to assess the effectiveness of the removal of the carbon contamination. The ratio O/Sn is used to confirm the stoichiometry.

These data indicate that the IPA cleaning process has little effect in removing organic contaminants. The ATM pressure plasma treatment is slightly more effective than the low-pressure vacuum plasma treatment for removing adventitious carbon. The O/Sn ratio shows that there is no significant change in the TEC 10 surface stoichiometry.

The low-pressure vacuum plasma treatment of TEC10 glass substrates decreased the WCA drastically to <10°. However, the WCA after the 5 min low-pressure plasma treatment is slightly higher than that achieved with the atmospheric-pressure plasma and

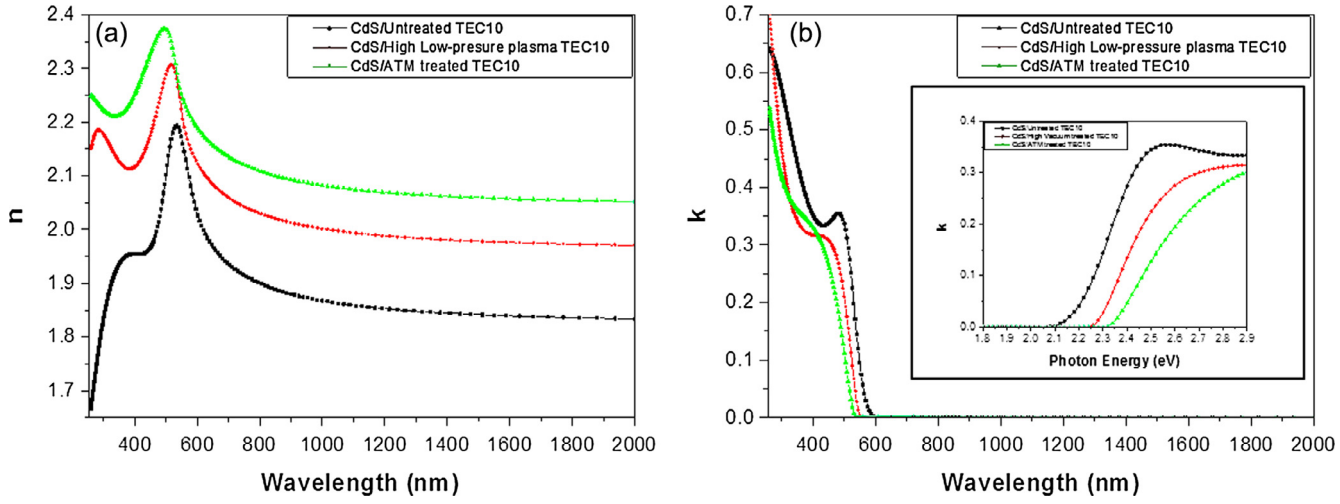

Fig. 9. Optical properties measured by spectroscopic ellipsometry of CdS thin films deposited on different substrates. (a) Refractive index. (b) Extinction coefficient. The inset in (b) shows the band gap shift towards higher eV for plasma treated substrates.

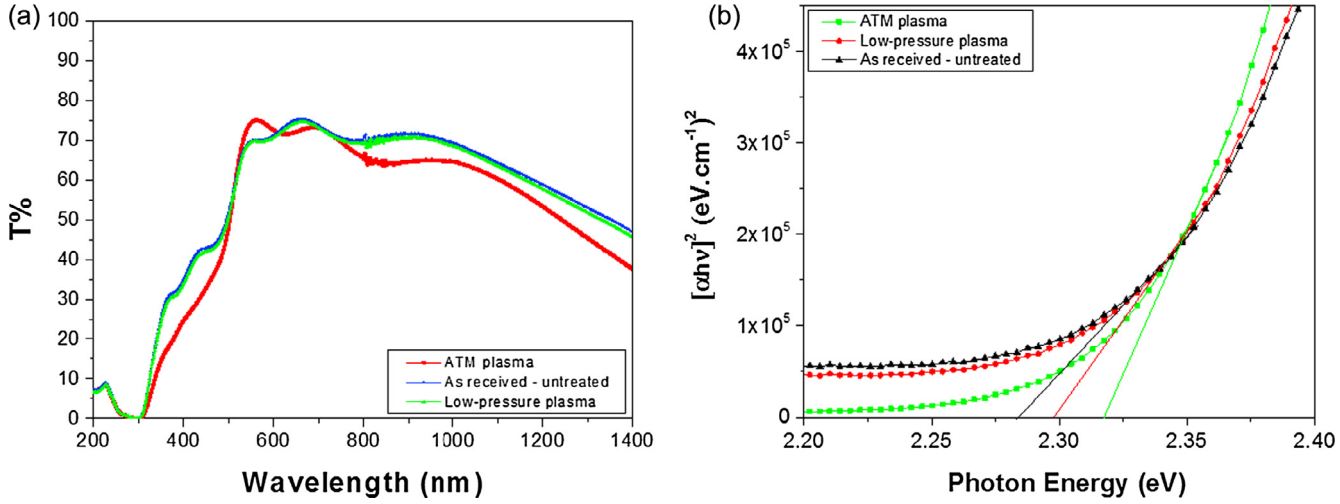

Fig. 10. (a) Transmittance curves of CdS thin films deposited on untreated TEC10, low pressure vacuum plasma treated and atmospheric-pressure plasma treated TEC10 glass. (b) Tauc plot and energy band gap estimation for CdS films deposited on untreated, low-pressure and atmospheric-pressure plasma treated TEC10 surfaces.

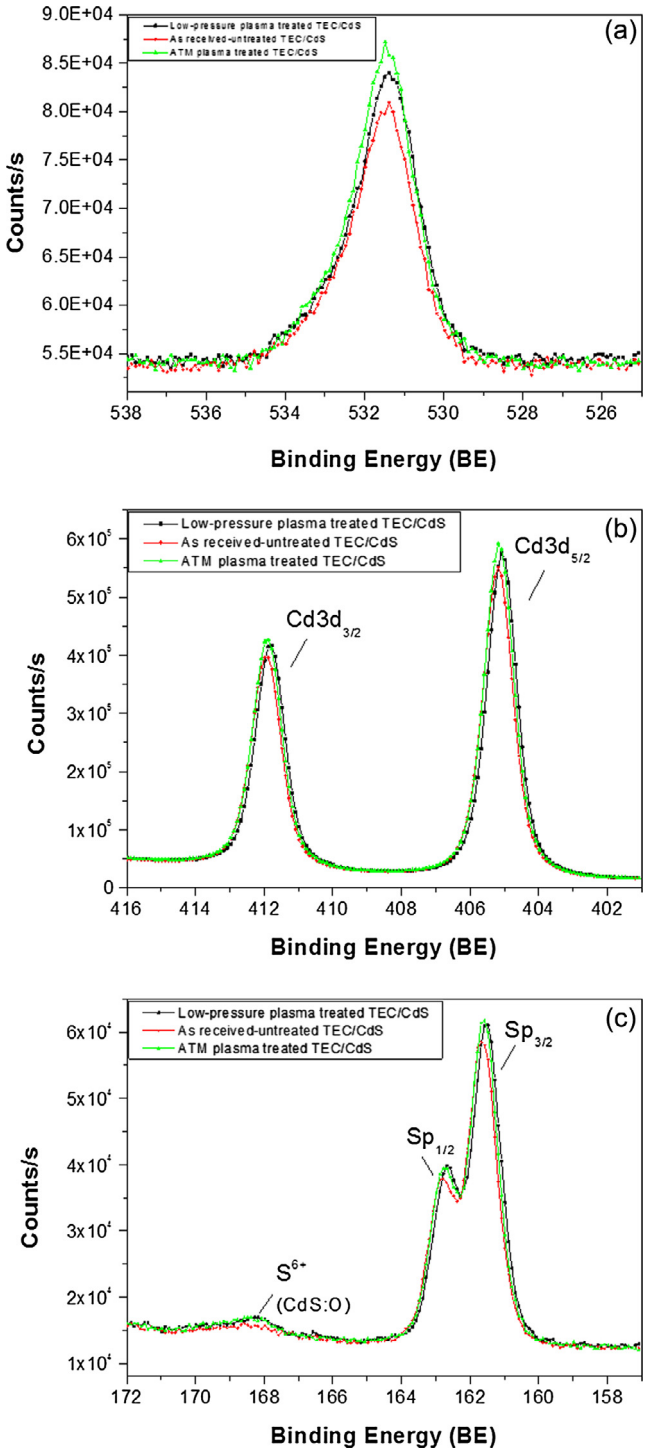

Fig. 11. XPS high resolution analysis of O1s (a), Cd3d (b) and S2p (c) peaks comparing CdS thin films grown on different substrates: untreated, low pressure vacuum plasma treated and atmospheric-pressure plasma treated TEC10 glasses.

the WCA recovers slightly faster. Nonetheless, both plasma treatments result in WCA less than 10° and the hydrophilicity is maintained after 24 h (WCA < 20°). This is shown in Fig. 4. The atmospheric-pressure plasma is slightly more effective than the low-pressure plasma cleaning, causing the largest decrease in the C1s peak and resulting in the lowest WCA. It also achieves these effects in the shortest treatment times. In contrast, the WCA measured on TEC10 glass immediately after cleaning with IPA resulted in WCA values of ~20°. It was deemed unnecessary to analyse the recovery of the WCA after the IPA wet treatment.

3.4. Properties of CdS thin films deposited on plasma treated substrates

We have demonstrated the effectiveness of an atmospheric-pressure plasma in removing surface contamination and activating the surface of SDL and TEC10 glass substrates. In this section, we analyse the properties of CdS thin films deposited on plasma treated substrates using sonochemical bath deposition (SonoCBD), a technique commonly used in the fabrication of thin film CdTe, CIGS and CZTS photovoltaic devices. The effect of the atmospheric-plasma pre-treatment on the adhesion, deposition rate and optical properties of the CdS films was examined. The CdS thin films were deposited for 30 min on untreated, low-pressure vacuum plasma cleaned and atmospheric-pressure plasma cleaned TEC10 glass surfaces.

3.4.1. Thin film CdS: Deposition rate and optical properties

Spectroscopic ellipsometry (SE) was used to obtain the optical properties and thickness of the CdS thin films. The Tauc-Lorentz model (see Section 2.4) (Fujiwara, 2007) was used to parameterise the spectral dependence of CdS refractive index (n) and extinction coefficient (k). Fig. 9 shows the derived optical properties for the CdS films deposited on untreated, low-pressure vacuum plasma treated and atmospheric-pressure plasma treated TEC10 substrates. CdS films deposited on treated surfaces show increased refractive index n (Fig. 9(a)) with the highest optical density obtained for the thin film deposited on the atmospheric-pressure plasma treated surface. The extinction coefficient (k) (Fig. 9(b)) has lower values for the CdS films deposited on atmospheric plasma treated surfaces. This is consistent with thin films with lower levels of contamination and fewer defects.

The deposition rate for the CdS thin film on the surface treated with the atmospheric-pressure plasma was 2.6 nm/min, (film thickness of ~80 nm) was approximately double the 1.3 nm/min deposition rate achieved on the IPA treated substrate (~40 nm film thickness). The deposition rate achieved for the low-pressure vacuum plasma treated substrate was 1.5 nm/min, (film thickness ~45 nm). As a result of the thicker film, the transmittance of the atmospheric-pressure plasma treated sample was slightly lower than that of the other samples despite having an improved extinction coefficient (Fig. 10(a)). The respective band gaps extracted using the Tauc plot (Fig. 10(b)) are in agreement with those obtained using ellipsometry (Fig. 9(b) and inset), and a shift towards higher energy is observed for the band gap of those films deposited on plasma cleaned substrates.

Table 2
C, Cd,O and S percentages detected by XPS scan surface analysis on CdS films to compare the untreated surface with high vacuum plasma and atmospheric plasma treated glass surfaces.

	C1s (%)	Cd3d (%)	O1s (%)	S2p (%)
Untreated/CdS	28.7	29.8	13.9	25.3
Low-pressure vacuum plasma/CdS	25.9	30.7	15.5	26.5
ATM-pressure plasma/CdS	21.9	32.2	17.1	26.8

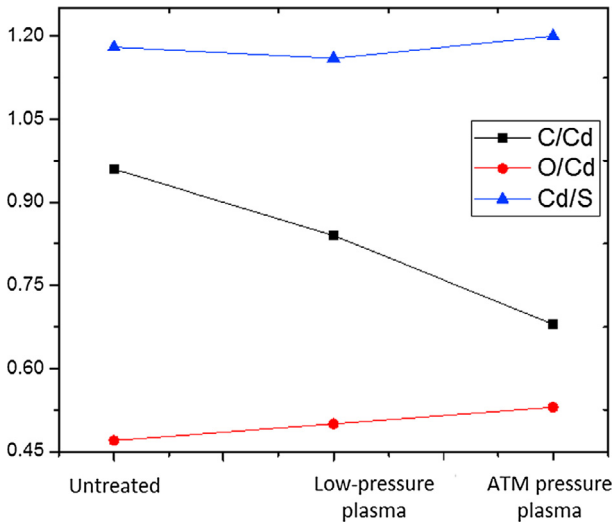

Fig. 12. XPS C/Cd, O/Cd and Cd/S ratios for a TEC 10 where no cleaning has been performed, TEC10 treated by low-pressure and ATM pressure plasma treatments.

The increase in the bandgap is consistent with the observed increase in the refractive index. The crystallinity of the films improves on the plasma cleaned substrates. The reduced density of defects results in an increase in the bandgap. The bandgaps measured using ellipsometry are slightly lower than the values obtained using the Tauc plot method (Fig. 9(b) inset and Fig. 10). The band gap has been extracted using the Tauc formula in the ellipsometric modelling (see Eq. (2)). The bandgap is defined as the point at which the extinction coefficient k is greater than zero. In the graphical method used in the Tauc plot, a tail of band states is neglected when extrapolating the transmittance.

3.4.2. Thin film CdS: surface composition

XPS analysis was performed on the CdS films deposited on untreated, low-pressure vacuum plasma treated and atmospheric-pressure plasma treated TEC10 glass. Fig. 11 shows the O1s, Cd3d and S2p peaks to compare the chemical composition of each CdS thin film surface. The O1s, Cd3d and S2p peaks of the CdS films are more intense in the pre-treated samples, with the highest intensities observed for the surface pre-treated with the atmospheric-pressure plasma. Table 2 shows the percentages of C, Cd, O and S detected on each sample. The ratios C/Cd, O/Cd and Cd/S are shown in Fig. 12. The reduction of carbon on the CdS films grown on the plasma treated surfaces did not alter the CdS stoichiometry. From the S2p spectra, the oxidation component at 168.3 eV corresponds to the formation of CdS:O with possible formation of $CdSO_4$ and/or $CdSO_3$. This is in agreement with the atomic compositional analysis shown in Table 2, where the O1s peak intensity increases for the treated substrates. The differences between the films are attributed to the different nucleation and growth conditions imparted by the surface pre-treatments that

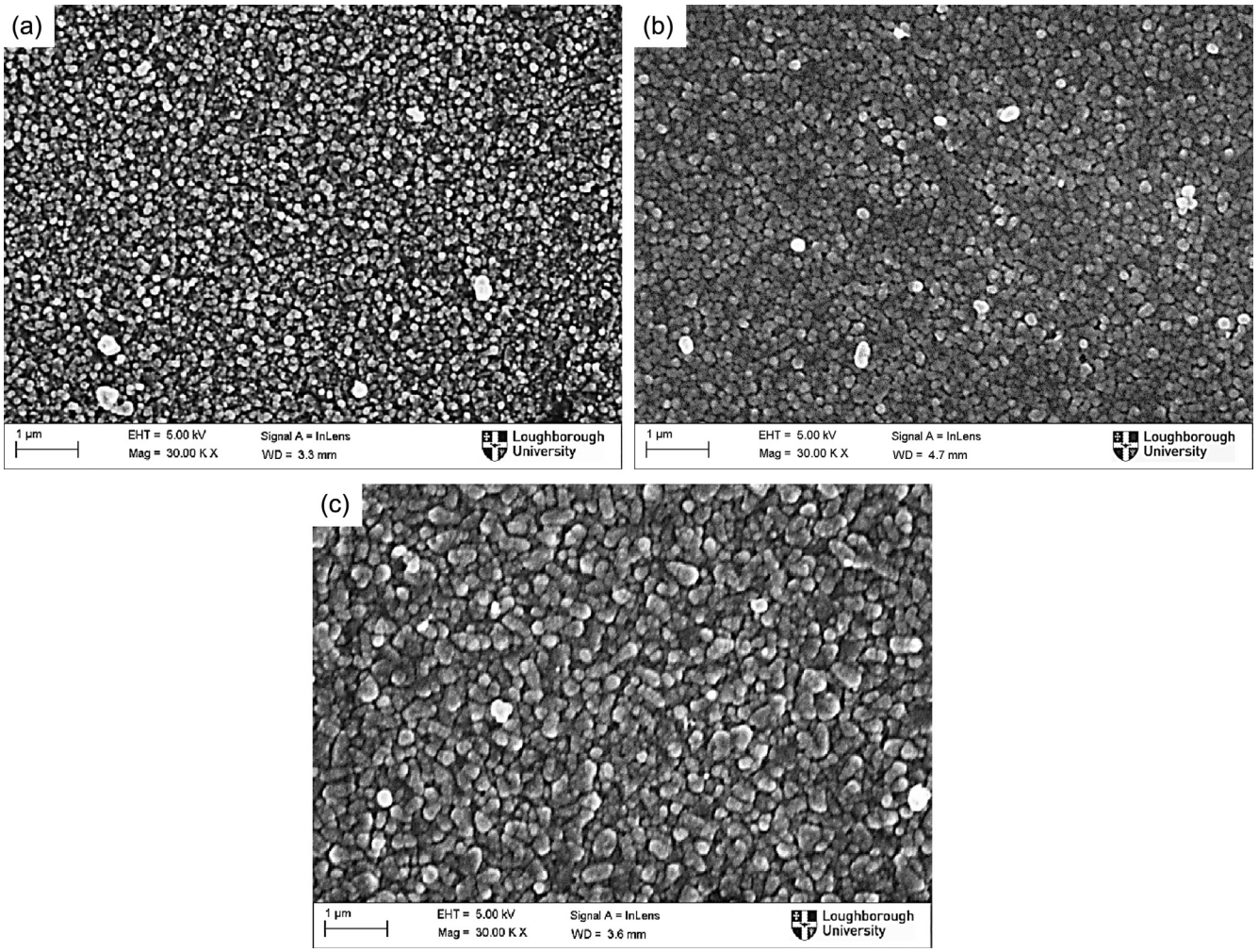

Fig. 13. SEM surface image of CdS thin film deposited on untreated (a) low-pressure vacuum plasma treated (b) and atmospheric-pressure plasma treated TEC10 glass (c).

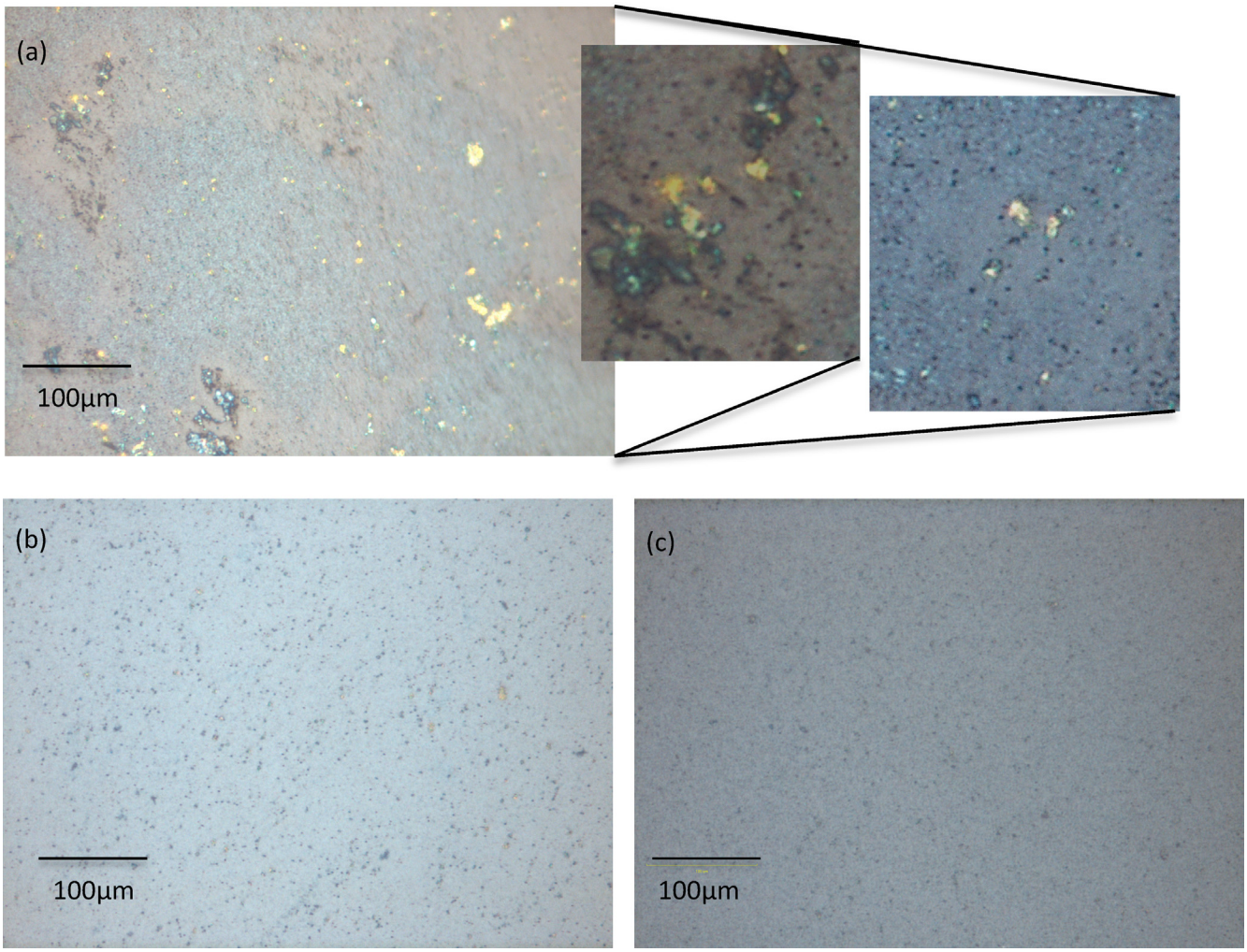

Fig. 14. Optical microscope images of pinholes, defects detected on three different areas of CdS films deposited on untreated TEC10 glass (a). As a comparison, the completely covered CdS layer deposited on high vacuum (b) and ATM pressure plasma treated TEC10 have shown (c).

lead not only to different growth rate, roughness and optical density but also to a different final surface composition.

3.4.3. CdS thin film CdS: Morphology and pinholes

The uniformity of the CdS layers deposited on atmospheric-pressure treated substrates was confirmed using SEM imaging (Fig. 13(c)). The films are free of voids and pinholes. The SEM images reveal the presence of uniform small crystallites. The grain size and the growth dynamics were affected by the substrate pre-treatment. The CdS thin films deposited on ATM pressure plasma treated TEC10 showed large crystallites ~200 ± 0.01 nm in size. The grain size of CdS films deposited on low-pressure vacuum plasma treated TEC10 is ~140 ± 0.01 nm. In comparison, the grain size of the CdS films deposited on the untreated substrate was much smaller ~100 ± 0.01 nm (Fig. 13(a)). The grain size was calculated as an arithmetic average over 10 measurements, by using the AxioVision LE64 software.

Optical microscopy was used to analyse the surface of the films and detect any pinholes or voids in the CdS thin films. Pinholes can be detected by using a light source deployed underneath the sample. If pinholes are present, bright spots appear in the images (Fig. 14). Voids were present in the CdS films deposited on untreated surfaces with a size measured to be ~3 ± 0.9 µm (as an average taken over 10 measurements). The CdS films deposited on atmospheric-pressure and low pressure vacuum plasma treated substrates appeared uniformly covered, and void and pinhole free. These results are consistent with the SEM images.

4. Conclusions

The volume of installations of photovoltaic modules increases as their cost is reduced. The cost of the energy produced by the modules is also reduced. Solution based deposition processes in atmosphere using inks or nanoparticles avoid the use of vacuum technology. The capital cost of vacuum systems is a significant barrier. However, the optimum production efficiency of a solution based manufacturing strategy can only be achieved if the entire module fabrication process is carried out in atmosphere. In this paper we report on an atmospheric-pressure plasma process that can be used for the surface activation of glass substrates. Surface pre-treatment is the crucial first process step to ensure good adhesion for thin film photovoltaic fabrication.

The use of an atmospheric-pressure plasma has been shown to be a highly effective treatment for the removal of adventitious organic contaminants and activation of substrate materials commonly used in photovoltaic device fabrication. The effectiveness of a mixed He and O_2 atmospheric-pressure plasma has been demonstrated using WCA and XPS analyses of treated soda lime glass and TEC10 glass substrates. When compared with a conventional wet cleaning process (ultrasonic IPA bath), the atmospheric-pressure plasma treatment was faster and more

effective. Surprisingly, it was also slightly more effective than and a low-pressure vacuum Ar/O_2 plasma cleaning process. The atmospheric-plasma process is more convenient to use.

The atmospheric-pressure plasma cleaning procedure is compatible with the atmospheric sonochemical CdS deposition process, enabling an effective vacuum-free route for CdS thin film deposition. It was found that the plasma treatment improves the thin film deposition rate as well as the density and compactness of the deposited CdS layers. Pinhole-free CdS thin films 80 nm in thickness were satisfactorily deposited on atmospheric-pressure plasma treated TEC10 substrates. The optical and morphological properties of the deposited thin films were consistent with increased film density with uniform CdS crystallites. Also, the atmospheric-pressure plasma treatment resulted in the subsequent growth of larger CdS grains. The average grain size on atmospheric plasma treated TEC10 surfaces was ~200 nm compared to ~100 nm for CdS layers deposited on untreated TEC10 glass.

Although, the use of atmospheric-pressure plasma provides a technique for effective surface pre-treatment, it does not remove gross contamination such as particles, so a wet cleaning process is still required for initial substrate preparation even if atmospheric plasmas are used in a manufacturing process. However, it is highly effective in removing adventitious carbon contamination and increasing surface energy. The effect of the surface pre-treatment is surprisingly long lived with low water contact angles still evident even after 24 h following the treatment.

The increase in surface energy, as evidenced by a decreasing water contact angle, improves thin film adhesion and also appears to improve the subsequent thin film growth by increasing film density and improving optical properties such as refractive index. Importantly, the use of atmospheric-pressure plasma is compatible with low cost atmospheric solution processing of thin film photovoltaic devices. It matches well with thin film deposition techniques such as electrodeposition, spin coating, spraying and printing. It is compatible with glass, metal or polymer substrates and could also be incorporated into a high volume process for flat panel substrates or in a roll-to-roll manufacturing system for flexible substrates. The technique will be useful as an initial process step for the solution processing of thin film CIS, CZTS, CIGS, and thin film organic-inorganic metal halide perovskite devices.

Acknowledgments

The authors are grateful to EPSRC and the RCUK Supergen SuperSolar Hub for financial support through grants EP/J017361/1 and EP/M014797/1.

References

Arnou, P., Van Hest, M.F.A.M., Cooper, C.S., Malkov, A.V., Walls, J.M., Bowers, J.W., 2016. Hydrazine-free solution-deposited CuIn(S, Se) 2 solar cells by spray deposition of metal chalcogenides. ACS Appl. Mater. Interf. 8, 11893–11897.

Baldwin, S., Bindewald, G., Brown, A., Chen, C., Cheung, K., 2015. Quadrennial Technology review An assessment of energy technologies and research Chapter 6: Innovating Clean Energy Technologies in Advanced Manufacturing.

Belkind, B.A., Gershman, S., 2008. Plasma cleaning of surfaces. Vac. Technol. Coat., 1–11

Cheng, A., Manno, M., Khare, A., Leighton, C., Campbell, S.A., Cheng, A., 2011. Imaging and phase identification of Cu2ZnSnS4 thin films using confocal Raman spectroscopy. J. Vac. Sci. Technol. A. 51203.

Deligianni, L., Ahmed, S., Romankiw, L.T., 2011. The Next Frontier: Electrodeposition for Solar Cell Fabrication.

Fauchais, P., Vardelle, A., 1997. Thermal plasmas. IEEE Trans. Plasma Sci. 25, 1258–1280.

Foster, J., Sommers, B.S., Gucker, S.N., Blankson, I.M., Adamovsky, G., 2012. Perspectives on the interaction of plasmas with liquid water for water purification. IEEE Trans. Plasma Sci. 40, 1311–1323.

Franssila, S., 2005. RCA-clean process. In: John Wiley & Sons (Ed.), Introduction to Microfabrication, pp. 301–303.

Fujiwara, H., 2007. Spectroscopic Ellipsometry Principles and Applications. Wiley, J. & Sons.

Gonçalves, D., Irene, E.A., 2002. Fundamentals and applications of spectroscopic ellipsometry. Quim. Nova 25, 794–800.

Hachioji-shi, 1987. Ultraviolet-Ozone Surface Treatment. Three Bond Tech. News, Tokyo, Japan.

Homola, T., Matousek, J., Medvecká, V., Zahoranová, A., Kormunda, M., Medvecká, V., Zahoranová, A., 2012. Atmospheric pressure diffuse plasma in ambient air for ITO surface cleaning. Appl. Surf. Sci., 1–6

Iza, F., Kim, G.J., Lee, S.M., Lee, J.K., Walsh, J.L., Zhang, Y.T., Kong, M.G., 2008. Microplasmas: sources, particle kinetics, and biomedical applications. Plasma Process. Polym. 5, 322–344.

Kim, H., Lee, J., Park, C., Park, Y., 2002. Surface characterization of o 2 -plasma-treated indium-tin-oxide (ITO) anodes for organic light-emitting-device applications. J. Korean Phys. Soc. 41, 395–399.

Kogelschatz, U., 2003. Dielectric-barrier Discharges: Their History, Discharge Physics, and Industrial Applications. Plasma Chem. Plasma Process 23, 1–46.

Kwoka, M., Ottaviano, L., Passacantando, M., Santucci, S., Czempik, G., Szuber, J., 2005. XPS study of the surface chemistry of L-CVD SnO_2 thin films after oxidation. Thin Solid Films 490, 36–42.

Lee, E.S., Choi, J.H., Baik, H.K., 2007. Surface cleaning of indium tin oxide by atmospheric air plasma treatment with the steady-state airflow for organic light emitting diodes. Surf. Coat. Technol. 201, 4973–4978.

Lisco, F., Abbas, A., Maniscalco, B., Kaminski, P.M., Losurdo, M., Bass, K., Claudio, G., Walls, J.M., 2014. Pinhole free thin film CdS deposited by chemical bath using a substrate reactive plasma treatment. J. Renew. Sustain. Energy 6, 11202–11209.

Liu, D., Rong, M., Wang, X., Iza, F., Kong, M.G., 2010. Main species and physicochemical processes in cold atmospheric-pressure He + O 2 plasmas. Plasma Process. Polym. 7, 846–865.

Low, B.L., Zhu, F.R., Zhang, K.R., Chua, S.J., 2002. An in situ sheet resistance study of oxidative-treated indium tin oxide substrates for organic light emitting display applications. Thin Solid Films 417, 116–119.

Mariotti, D., Belmonte, T., Benedikt, J., Velusamy, T., Jain, G., 2016. Low-temperature atmospheric pressure plasma processes for "'Green'" third generation photovoltaics. Plasma Process. Polym. 13, 70–90.

Massines, F., Sarra-bournet, C., Fanelli, F., Gherardi, N., 2012. Atmospheric pressure low temperature direct plasma technology: status and challenges for thin film deposition. Plasma Process. Polym. 9, 1041–1073.

Menzel-Gläser_ Microscope Slides [WWW Document], n.d. URL <http://www.menzel.de/Microscope_Slides.687.0.html?L=1>.

Mitzi, D.B., Yuan, M., Liu, W., Kellock, A.J., Chey, S.J., Deline, V., Schrott, A.G., 2008. A High-efficiency solution-deposited thin-film photovoltaic device. Adv. Mater. 20, 3657–3662.

Morent, R., De Geyter, N., Verschuren, J., De Clerck, K., Kiekens, P., Leys, C., 2008. Non-thermal plasma treatment of textiles. Surf. Coat. Technol. 202, 3427–3449.

NIST X-ray Photoelectron Spectroscopy Database, Version 4.1 [WWW Document], 2012. Natl. Inst. Stand. Technol. Gaithersbg. URL <http://srdata.nist.gov/xps/>.

Rakhshani, A., 2000. Study of Urbach tail, bandgap energy and grain-boundary characteristics in CdS by modulated photocurrent spectroscopy. J. Phys. Condens. Matter 12, 4391–4400.

Samanta, K., Jassa, M., Agrawal, A.K., 2006. Atmospheric pressure glow discharge plasma and its applications in textile. Indian J. Fibre & Textile Res. 3, 83–98.

Schutze, A., Jeong, J.Y., Babayan, S.E., Park, J., Selwyn, G.S., Hicks, R.F., 1998. The atmospheric-pressure plasma jet: a review and comparison to other plasma sources. IEEE Trans. Plasma Sci., 1685–1694

Selwyn, G.S., Herrmann, H.W., Park, J., Henins, I., 2001. Materials processing using an atmospheric pressure, RF-generated plasma source. Contrib. Plasma Phys. 6, 610–619.

Shaw, A., Shama, G., Iza, F., 2015. Emerging applications of low temperature gas plasmas in the food industry. Biointerphases, 0–25.

Sherman, R., Hirt, D., Vane, R., 1994. Surface cleaning with the carbon dioxide snow jet. J. Vac. Sci. Technol. A Vacuum, Surfaces, Film 12, 1876–1881.

Slyke, S.A., Chen, C.H., Tang, C.W., Van Slyke, S.A., Chen, C.H., Tang, C.W., 1996. Organic electroluminescent devices with improved stability Organic electroluminescent devices with improved stability. Appl. Phys. Lett. 69, 1–4.

Suryawanshi, M.P., Agawane, G.L., Bhosale, S.M., Shin, S.W., Patil, P.S., Kim, J.H., Moholkar, A.V., 2013. CZTS based thin film solar cells: a status review. Mater. Technol. 28, 98–109.

Swanson, D.E., Lutze, R., Sampath, W., Williams, J.D., 2012. Plasma cleaning of TCO surfaces prior to CdS/CdTe deposition. In: 38th Photovolt. Spec. Conf. Conf. (PVSC), 2012. IEEE, pp. 859–863.

Thejaswini, H.C., Hoskinson, A.R., Agasanapura, B., Grunde, M., Hopwood, J., 2014. Diamond & Related Materials Deposition and characterization of diamond-like carbon films by microwave resonator microplasma at one atmosphere. Diam. Relat. Mater. 48, 24–31.

Walsh, J.L., Iza, F., Janson, N.B., Law, V.J., Kong, M.G., 2010. Three distinct modes in a cold atmospheric pressure plasma jet. J. Phys. D. Appl. Phys. 43, 1–14.

Walsh, J.L., Shi, J.J., Kong, M.G., 2006. Contrasting characteristics of pulsed and sinusoidal cold atmospheric plasma jets. Appl. Energy 88, 1–3.

Wangperawong, A., King, J.S., Herron, S.M., Tran, B.P., Pangan-Okimoto, K., Bent, S.F., 2011. Aqueous bath process for deposition of Cu2ZnSnS4 photovoltaic absorbers. Thin Solid Films 519, 2488–2492.

Von Woedtke, T., Reuter, S., Masur, K., Weltmann, K., 2013. Plasmas for medicine. Phys. Rep. 530, 291–320.